Water Tree Influence on Space Charge Distribution and on the Residual Electric Field in Polyethylene Insulation

Cristina Stancu*, P. V. Notingher**, P. Notingher jr***, M.Plopeanu**

*INCDIE ICPE CA, 313 Splaiul Unirii, P.O. Box 149, Bucharest 030138, Romania,
E-Mail: cstancu@icpe-ca.ro

**Politehnica University of Bucharest, Splaiul Independentei St., No.313, 060042,
Bucharest, Romania, E-Mail: petrunot@elmat.pub.ro, mgplopeanu@elmat.pub.ro

***Université Montpellier 2, Institut d'Electronique du Sud, Groupe Energie et Matériaux,
Place E. Bataillon, CC 083, 34095 Montpellier Cedex 5, France, E-Mail: petru@univ-montp2.fr

Abstract - ***A computation method of the electric field and ionic space charge density in plane insulations with water trees (using a Comsol Multiphysics software and the thermal step currents ($I_m(t)$) measured with Thermal Step Method) is presented. A parabolic spatial variation of volume charge density, an exponential spatial variation of the electric permittivity ε and a linear dependency of ε and the temperature coefficient of permittivity α_ε with the average water concentration in trees, are considered. For a water tree with a known length, different values of charge density are considered and the electric field and the thermal step currents $I_c(t)$ are calculated. The currents $I_c(t)$ and $I_m(t)$ are compared and the volume of charge density and electric field for which $I_c(t)$ is identical with $I_m(t)$ are kept.***

***Key words*: insulation systems, electric field, space charge, water trees**

I. INTRODUCTION

One of the main causes of premature breakdown of average and/or high voltage electrical insulation is the existence of local electric fields exceeding the inception values of partial discharges and electrical treeing. The local intensification of the electric field is due to conductor defects (sharp edges, protrusions etc), insulation defects (delamination, cavities etc), electrochemical trees (water, cooper, etc) [1].

In the case of polyethylene insulated power cables, water trees develop either in the vicinity of bulk defects (bow tie trees), or from inner and/or outer semi-conducting layers (vented trees) and they appear under the shape of micro cavities filled with water connected by very thin micro channels [2], [3]. Water treeing leads to ionic space charge formation (corresponding to the salt dissolved in water), inside and outside the treed regions, the quantity depending on the salt concentration in water, on water trees dimensions, frequency of the electric field etc [5], [6].

In previous papers [7]…[9], correlations between the water trees length l_a and average space charge density ρ_v have been shown. In the present paper a computation method of the electric field and space charge on the basis of measured thermal step current in insulations with water trees is presented. A Comsol software is used and the dependencies of permittivity ε and temperature coefficient of permittivity α_ε as a function of their average values (corresponding to polyethylene and water) and average water concentration in trees are taken into consideration.

II. THERMAL STEP METHOD

The thermal step method (TSM) consists in the application of a thermal step ΔT (Figure 1) on one face of the tested sample situated between two electrodes [10]. As a consequence, the space charge inside the sample, moves, the induced charges on electrodes are modified, and by connecting the electrodes in short-circuit a current $I(t)$ appears, having the expression [11]:

$$I(t) = -C \int_{y_0}^{y} \alpha_\varepsilon(y) E(y) \frac{\partial T(y,t)}{\partial t} \mathrm{d}y \, , \qquad (1)$$

where α_ε is the temperature coefficient of permittivity, C – the sample capacity before the thermal step application, $E(y)$ – the electric field strength in coordinate point y (perpendicular measured on the electrodes surfaces), $T(y,t)$ – the temperature value in coordinate point y at instant t, y_0 – a computation quantity depending on the electrode characteristics which is in contact with the liquid which generates the thermal wave.

By measuring the current $I(t)$ and using equation (1), the values of electric field $E(y)$ and volume space

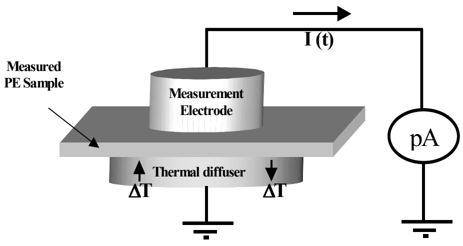

Fig. 1. Setup used for the thermal step current measurement.

charge density $\rho_v(y)$ can be calculated in each point of the tested sample.

If in the case of homogeneous samples, ε and α_ε are known constants, their values are relatively difficult to determine in the case of water treed insulations. On the basis of some experimental data, different variations laws with the *y* coordinate have been proposed for ε: linear, parabolic, exponential etc. [12] …[14]. In the present paper an exponential variation law of permittivity was considered:

$$\varepsilon_r(y) = c\mathrm{e}^{-dy}, \qquad (2)$$

where $\varepsilon_r(y)$ is the relative permittivity in coordinate point *y*, and *c* and *d* are material constants.

The α_ε coefficient values were deduced on the basis of permittivity variation curves of polyethylene and water with temperature between -5 ºC and 25 ºC [15]...[17]. The obtained values are $\alpha_{\varepsilon PE} = 4.4\cdot10^{-4}$ K^{-1} for polyethylene and $\alpha_{\varepsilon w} = -\ 7.26\cdot10^{-3}$ K^{-1} for water. For water treed regions a average coefficient $\alpha_{\varepsilon m}$ was calculated:

$$\alpha_{\varepsilon m} = c_{wm}\alpha_{\varepsilon w} + (1 - c_{wm})\alpha_{\varepsilon PE}, \qquad (3)$$

where c_{wm} is the average water concentration [18]…[20].

Because the water concentration decreases exponentially from the base towards the front of water trees [19], we considered for α_ε the same kind of variation like permittivity:

$$\alpha_\varepsilon(y) = c_1\mathrm{e}^{d_1 y}, \qquad (4)$$

where the constants c_1 and d_1 are material constants.

III. ELECTRIC FIELD COMPUTATION

Let us consider a flat sample which has the diameter *d* and the thickness *g*, situated between the ground electrode and the thermal diffuser (Fig. 1). It is supposed that from the sample face which is in contact with the thermal diffuser a continuous water tree with the length l_a has developed, to whom corresponds an ionic space charge layer of volume density $\rho_v(y)$ and thickness l_s ($l_s > l_a$). This charge generates an electric field of intensity *E*. As the electric field has a plane parallel symmetry, it can be computed in a rectangular domain *D* (resulting from the division into sections of the disc with a perpendicular plane on its basis). The domain *D* is constitued of 4 sub-domains $D_{1\ldots4}$, delimited by the boundaries 1…13 (Fig. 2):

- Sub-domain D_1 – corresponding to the thermal diffuser/sample area, whose thickness y_0 is experimentally determined and where the electric field in zero;
- Sub-domain D_2 – corresponding to the water treed region with the length l_a ($\varepsilon_r\ (T,y) = (1+\alpha_\varepsilon(y)\cdot(T - T_0))\cdot c\mathrm{e}^{-dy}$) and with a space charge layer with the thickness $l_s - l_a$ and $\rho_v(y) = \rho_{v0}(ay^2 + by + e)$;
- Sub-domain D_3 – corresponding to the region without trees ($\varepsilon_r\ (T) = \varepsilon_{rPE}\ (1+\alpha_{\varepsilon PE}(T - T_0))$) and a space charge layer l_s with $\rho_v(y) = \rho_{v0}(ay^2 + by + e)$;
- Sub-domain D_4 – corresponding to the region without water trees ($\varepsilon_r\ (T) = \varepsilon_{rPE}\ (1+\alpha_{\varepsilon PE}(T - T_0))$) and without space charge.

Considering that y_0, l_a, l_s, ρ_{v0}, *a*, *b*, *c*, c_1, *d*, d_1, *g*, $\alpha_{\varepsilon PE}$ and $\alpha_{\varepsilon w}$ are known, using the Comsol Multiphysics software, the electric field repartition and temperature in domain *D* were determined. Knowing the initials and boundaries conditions for electric potential $V(y)$ and temperature $T(y,t)$, the Poisson equation for electric field $\Delta V = -\ \rho_v/\varepsilon$ and Fourier equation for temperature $\gamma c_p \partial T/\partial t = \mathrm{div}(\lambda \mathrm{grad} T)$ where γ is the density, c_p - specific heat and λ - thermal conductivity, were solved. In all sub domains, an initial temperature of 25 °C was considered. At the instant $t = 0$, the temperature on boundary 1 decreases to -5 °C, corresponding to the application of a thermal step $\Delta T = -\ 30$ °C. It is considered that the thermal wave acts a time *t* ($t = 5$ s) divided into several intervals ($\Delta t = 5$ ms).

The boundaries conditions are:

- $V = 0$ on boundaries 1, 2, 3, 4 and 13,

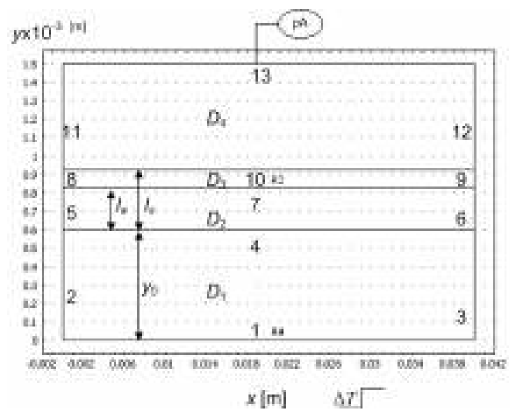

Fig. 2. Computational domain of the electric field.

- $\overline{nE} = 0$ on boundaries 5, 6, 8, 9, 11 and 12,
- $(\varepsilon E_n)_2 = (\varepsilon E_n)_3$ on boundary 7,
- $(\varepsilon E_n)_3 = (\varepsilon E_n)_4$ on boundary 10,

where $\bar{n}$ is the surface normal and E_n the normal component of E.

The values of the density (γ), thermal conductivity (λ) and specific heat (c_p) corresponding to the water trees regions have been computed on the basis of the polyethylene and water values, by using a similar equation with (4), for different quantities of average water concentration c_{wm} (Table 1).

TABLE 1. Values for different average water concentration in polyethylene c_{wm} (l_a = 227 μm).

c_{wm} [%]	γ [kg/m^3]	λ [W/mK]	c_p [J/kgK]	$\alpha_{\varepsilon m}$ 10^4 [K^{-1}]	ε_{rm}
0	930	0.38	1900	4.4	2.3
1	930.7	0.382	2318.8	3.63	3
1.5	931.05	0.383	2328.2	3.24	3.5
2	931.4	0.384	2337.6	2.86	3.9

Material constants c, c_1, d and d_1 are computed from the equations (5) and (6):

$$\varepsilon_r (y_0 + l_a) = \varepsilon_{rPE}$$
$$\int_{y_0}^{y_0+l_a} \varepsilon_r(y)\mathrm{d}y = \varepsilon_{rm} . l_a \qquad (5)$$
$$\varepsilon_{rm} = c_{wm}\,\varepsilon_{rw} + (1 - c_{wm})\,\varepsilon_{rPE},$$

$$\int_{y_0}^{y_0+l_a} \alpha_\varepsilon(y)\mathrm{d}y = \alpha_{\varepsilon m} l_a \qquad (6)$$
$$\alpha_\varepsilon(y_0+l_a) = \alpha_{\varepsilon PE},$$

where l_a is the tree length (assumed as continuous), c_{wm} and ε_{rm} - the average water concentration and the average permittivity of the treed zone, and ε_{rw} and ε_{rPE} - the relative permitivitties of water and polyethylene.

The thermal step current corresponding was computed using the relation:

$$I_c(t) = -\varepsilon S \frac{\mathrm{d}E_1}{\mathrm{d}t}, \qquad (7)$$

where ε is the absolute permittivity of sample, S - the electrode area, and E_1 - the electric field in the vicinity of measuring electrode (boundary 13, Fig. 2).

IV. EXPERIMENTS

A. Samples

The experiments were made on flat samples having the dimensions 100x100x0.5 mm^3, made from LDPE pellets by pressmoulding at p = 200 bar and T = 145 °C. In the samples, water trees were developed in an accelerated manner. For electrical measurements, graphite electrodes (40 mm in diameter) have been deposited. For measuring the trees lengths, the samples were cut in slices of 200 μm.

B. Setups

The setup used for water trees development is presented in Fig. 3 [8]. The applied effective voltage was U = 2 kV, the frequency - f = 5 kHz, the NaCl concentration in water - c = 0.1 mol/l, and the duration of voltage application - τ = 0…48 h. For measuring the dimensions of the water trees, the experimental setup presented in Fig. 4 was used.

V. RESULTS. DISCUSSIONS

A. Thermal step current measurement

The variations of the thermal step currents in samples without and with water trees of the length l_a (Fig. 5) are presented in Figure 6. It can be observed that the maximum values of thermal step currents $I_{m,\max}$ are higher in water treed samples with respect to virgin samples. For l_a = 0, 157 and 227 μm, the values of $I_{m,\max}$ are 8, 44 and 152 pA respectively. This is due to ionic space charge accumulation in the samples - resulted from the dissociation of NaCl molecules, which is more important in the last samples.

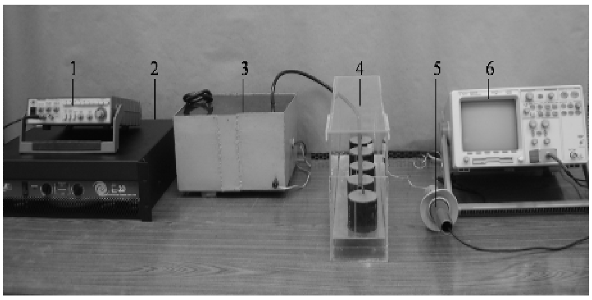

Fig. 3. Setup for accelerated water tree development: (1)– Generator, (2) – Amplifier, (3) – Transformer, (4) – Sample holder, (5) – Probe, (6) – HP Scope.

Fig. 4. Setup for measuring the water trees dimensions: (1) – PC, (2) – Camera, (3) – Microscope, (4) – Monitor.

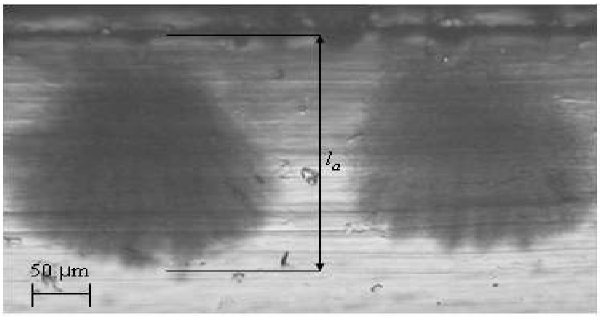

Fig. 5. Water trees developed in LDPE samples
(τ = 48 h, U = 2 kV, f = 5 kHz).

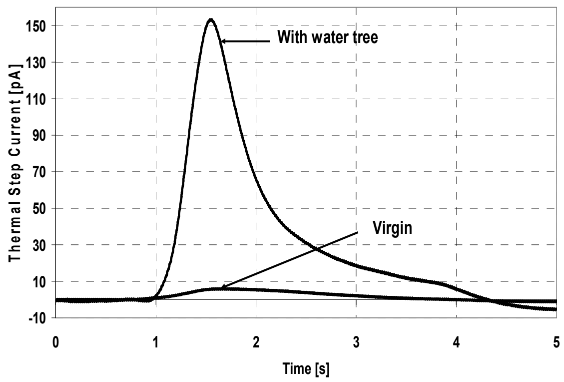

Fig. 6. Thermal step currents $I_m(t)$, measured on samples with and without water trees.

B. Computation of thermal step currents and electric field

Considering different values of ρ_{v0} (- 4.4...- 2.7 C/m^3) and l_s (267... 327 μm), thermal step currents $I_c(t)$ for values of t between 0 and 5 s were computed using the Comsol software. The obtained curves $I_c(t)$ were compared with the experimental one $I_m(t)$ to find the values of ρ_{v0} and l_s for which $I_m(t) \approx I_c(t)$.

Fig. 7 shows the variation of the maximum values of electric field strength E with ρ_{v0} and l_s. It can be seen that $E_{\max}$ decreases with the increase of l_s and increases with the increase of ρ_{v0}, variations which are similar to the ones obtained in the case of average voltage cables [8].

Fig. 8 shows the time variation of the computed thermal step current $I_c(t)$ for different values of the temperature coefficient of permittivity α_ε. As expected the decrease of $\alpha_\varepsilon(y)$ in D_2 causes a decrease in the thermal step current (curve 2, Fig. 8). This decrease becomes even more important in the case where α_ε varies exponentially (curve 3, Fig. 8).

In Fig. 9 the thermal step current $I_m(t)$ - measured on a water treed sample - and the thermal step current $I_c(t)$ simulated in water treed samples for which it has assumed l_a = 227 μm, l_s = 327 μm, y_0 = 0.6 mm and

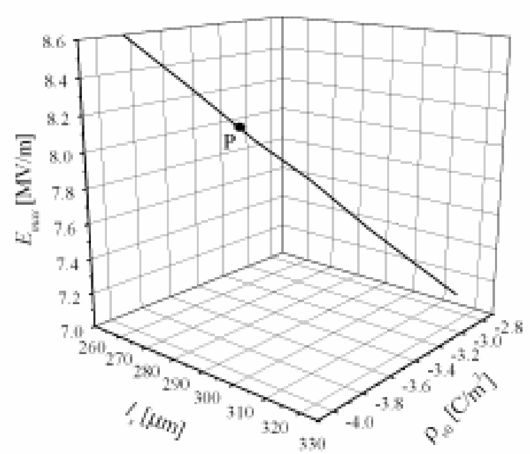

Fig. 7. Maximum electric field $E_{\max}$ vs l_s and ρ_{v0}
(l_a = 227 μm, $\alpha_{\varepsilon PE}$ = 4.4 ·10^{-4} K^{-1}, y_0 = 0.21 mm).

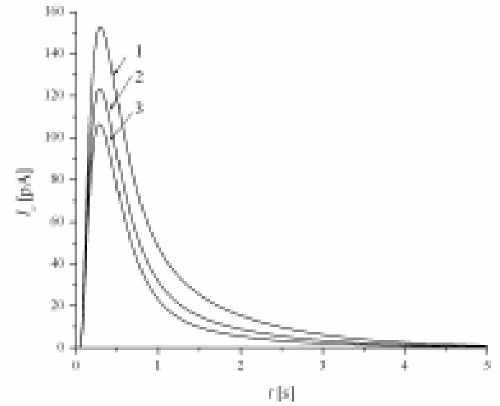

Fig. 8. Computed current time variation $I_c(t)$ in D_2 for $\alpha_{\varepsilon PE}$ = 4.4· 10^{-4} K^{-1} (1), $\alpha_{\varepsilon m}$ = 3.63· 10^{-4} K^{-1} (2), and $\alpha_\varepsilon(y) = c_1 e^{d_1 y}$ (3), (l_a = 227 μm, l_s = 327 μm).

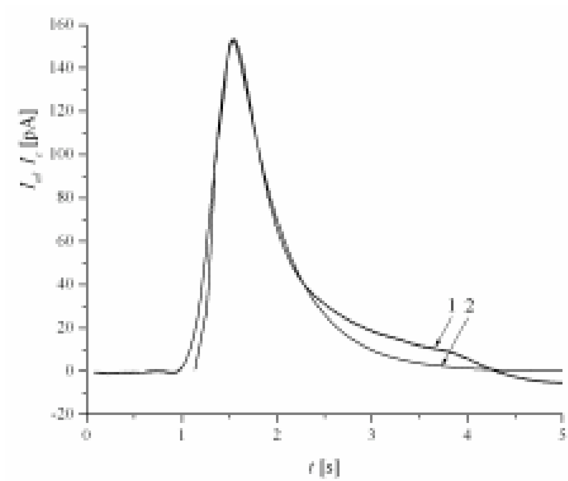

Fig. 9. Measured $I_m(t)$ (1) and computed $I_c(t)$ (2) thermal step currents for l_a = 227 μm and l_s = 327 μm.

ρ_{v0} = - 2.71 C/m^3 and $\alpha_{\varepsilon PE}$ = 4.4 ·10^{-4} K^{-1}, or ρ_{v0} = - 3.35 C/m^3 and $\alpha_\varepsilon(y) = c_1 e^{d_1 y}$ are presented. It can be observed that the decrease of the values of α_ε, due to water penetration inside the samples, leads to the increase of space charge density ρ_{v0} (from - 2.71 C/m^3 in the absence of the water trees to - 3.35 C/m^3 in their presence).

Electrical field variation vs *y*-coordinate, for different values of α_ε, in the water treed area is shown in Fig. 10. It is remarked that the α_ε decrease in D_2 causes an increase in E (curve 2, Fig. 10), and that this increase becomes more important in the case where α_ε varies exponentially (curve 3, Fig. 10).

In Figs. 11 and 12 the variations of electric field and volume space charge density (with the *y* - coordinate), for different values of the average water concentrations are presented. It can be observed that the electric field E and volume space charge density have important variations in the vicinity of the regions from where the water trees develop, and decrease with the *y*-coordinate, as a consequence of the decrease of ion concentration related to water trees [4].

It must be also remarked that the increase of the average water concentration values c_{wm} determines an increase of E and ρ_v values (Figs. 11, 12 and 13). Consequently, the values of residual electric field in the vicinity of samples faces from where water trees develop are relatively important (over 11 kV/mm in the case of a tree with a average water concentration c_{wm} = 1 %), and increases if the water concentration increases (due to the increase of space charge density related to water trees). For example, if the average water concentration in the trees reaches 2.4 %, the value of $E_{\max}$ reaches to 18 kV/mm (enough to initiate an electrical tree [21]).

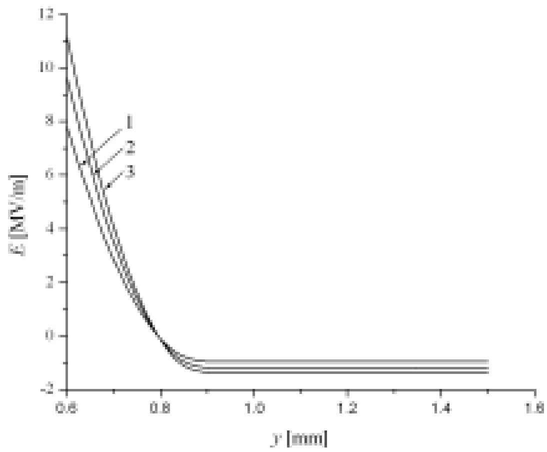

Fig. 10. Electrical field variation E vs *y*-coordinate for $\alpha_{\varepsilon PE} = 4.4\cdot 10^{-4}$ K^{-1}, ρ_{v0}= - 2.71 C/m^3 (1), $\alpha_{\varepsilon m}$ = 3.63· 10^{-4} K^{-1} (in D_2), ρ_{v0}= - 3.35 C/m^3 (2) and $\alpha_\varepsilon(y) = c_1 e^{d_1 y}$ (in D_2), ρ_{v0}= - 3.9 C/m^3 (3) (l_a = 227 µm, l_s = 327 µm).

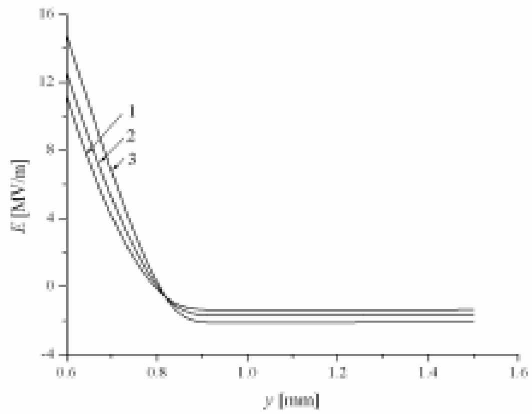

Fig. 11. Electrical field variation E vs *y* - coordinate for different average water concentrations c_{wm}: c_{wm} = 1 % (1), c_{wm} = 1.5 % (2), and c_{wm} = 2 % (3), ($\alpha_\varepsilon(y) = c_1 e^{d_1 y}$, l_a = 227 µm, l_s = 327 µm, y_0 = 0.6 mm).

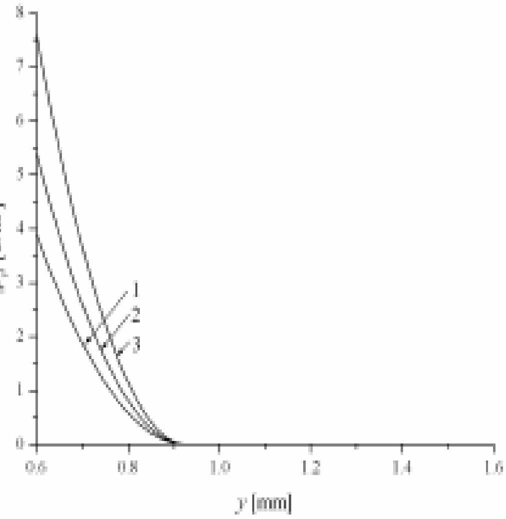

Fig. 12. Space charge density variation ρ_v vs *y*-coordinate for different average water concentrations c_{wm}: c_{wm} = 1 % (1), c_{wm} = 1.5 % (2), and c_{wm} = 2 % (3), ($\alpha_\varepsilon(y) = c_1 e^{d_1 y}$, l_a = 227 µm, l_s = 327 µm, y_0 = 0.6 mm).

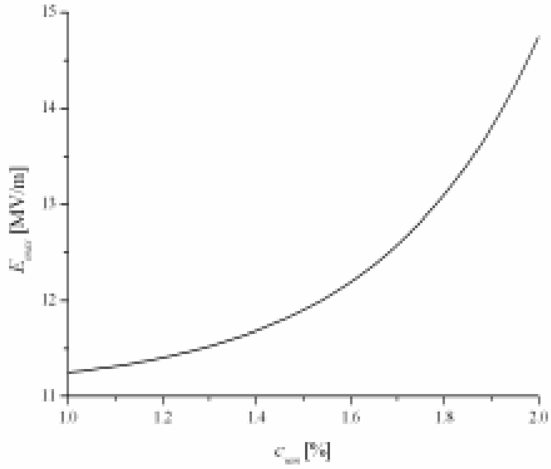

Fig. 13. Maximum electrical field intensity variation $E_{\max}$ with average water concentration in trees c_w ($\alpha_\varepsilon(y) = c_1 e^{d_1 y}$, l_a = 227 µm, l_s = 327 µm, y_0 = 0.6 mm).

V. CONCLUSIONS

The computational method presented in this paper evaluates in a good manner the residual electric field in water treed flat samples. The maximum values of the electric field depend on the space charge layer thickness l_s and on the volume space charge density ρ_{v0}.

The increase of average water concentration determines an increase of the permittivity ε_r and a decrease of the temperature coefficient of permittivity α_ε. Therefore the values of the computed current $I_c(t)$ decrease. On the other hand, the increase of water content in the trees results in an increase of maximum values of charge density ρ_{v0} and electric field $E_{\max}$.

In the inception areas of the water trees, the values of the residual electrical field generated by the water trees related ionic space charge may be significant in the case of high average water concentration in water trees (over 18 MV/m for c_{wm} = 2.4 %). Therefore, partial discharges and water trees which were initiated when the insulation was in use can develop even after the voltage was stopped.

ACKNOWLEDGEMENT

This work was supported in part by the Romanian Ministry of Education, Research and Youth, PNCDI II Program.

REFERENCES

[1] L.A. Dissado, J.C. Fothergill, "Electrical degradation and breakdown in polymers", Peter Pelegrinus, London, 1992.

[2] J.L. Chen, J.C. Filipini, "The morphology and behavior of the water tree", IEEE Transactions on Dielectrics and Electrical Insulation, vol. 28, 2, pp. 271–286, 1993.

[3] E.F. Steennis, F.H. Kreuger, "Water treeing in polyethylene cables", IEEE Transactions on Dielectrics and Electrical Insulation, vol. 35, 5, pp. 989 -1028, 1990.

[4] O.Visata, "*Influence des arborescences d'eau sur les propriétés diélectriques des polymères*", Thesis, University POLITEHNICA of Bucharest - University Joseph Fourier, Grenoble, 2001.

[5] T.Takada, "Acoustic and optical methods for measuring electric charge distributions in dielectrics", IEEE Transactions on Dielectrics and Electrical Insulation, vol. 6, 5, pp. 519-547, 1999.

[6] Y. F. F. Ho, G. Chen, A. Davies, E. Swingler, S. Sutton, N. Hampton, S. Hobdell, "Measurement of space charge in XLPE insulation under 50 Hz AC electric stresses using the LIPP method", IEEE Transactions on Dielectrics and Electrical Insulation, vol. 9, 3, pp. 362-370, 2002.

[7] C. Stancu, P.V. Notingher, F. Ciuprina, P. Notingher jr, S. Agnel, J. Castellon, A. Toureille, "Electric field computation in water treed polyethylene with space charge accumulation", Conference Record of The 2006 IEEE International Symposium on Electrical Insulation, Toronto, pp. 186 – 189, 2006.

[8] C. Stancu, P.V. Notingher, F. Ciuprina, P. Notingher jr, S. Agnel, J. Castellon, A. Toureille, "Computation of the electric field in cable insulation in the presence of water trees and space charge", IEEE Transactions on Industry Applications, vol. 45, 1, pp. 30-43, 2009.

[9] C. Stancu, "*Caracterisation de l'etat de vieillissement des isolations polymeres par la mesure d'arborescences et de charges d'espace*", Thesis, University Politehnica of Bucharest – University Montpellier 2, 2008.

[10] A. Toureille, A. Sabir, J. Reboul, J. Berdala, P. Merle, "Determination des densites de charge d'espace dans un cable haute tension a forte epaisseur d'isolant par la methode de l'onde thermique", Revue de Physique Appliquee, vol. 25, 4, pp. 405-408, 1990.

[11] A. Cernomorcenco, P. Notingher jr., "Application of the thermal step method to space charge measurements in inhomogeneous solid insulating structures: A theoretical approach", Applied Physical Letters, vol. 93, 19, 2008.

[12] I. Radu, M. Acedo, P.V. Notingher, F. Frutos, J.C. Filippini, "The danger of water trees in polymer insulated power cables evaluated from calculations of electric field in the presence of water trees of Different Shapes and Permittivity Distributions", Journal of Electrostatics, vol. 40-41, pp. 343-347, 1997.

[13] I. Radu, M. Acedo, J.C. Filippini, P.V. Notingher, F. Frutos, "The effect of water treeing on the electric field distribution of XLPE: consequences on the dielectric strength", IEEE Transactions on Dielectrics and Electrical Insulation, vol. 7, 6, pp. 860-868, 2000.

[14] M. Acedo, I. Radu, F. Frutos, J.C. Filippini, P.V. Notingher, "Water treeing in underground power cables: modelling of the trees and calculation of the electric field perturbation", Journal of Electrostatics, vol. 53, pp. 267-294, 2001.

[15] I. Alig, S.M. Dudkin, W. Jenninger, M. Marzantowicz, "AC Conductivity and dielectric permittivity of poly (ethyleneglycol) during crystallization: percolation picture", Polymer, vol. 47, pp. 1722-1731, 2006.

[16] V. Svorcik, O. Ekrt, V. Rybka, J. Liptak, V. Hnatowicz, "Permittivity of polyethylene and polyethylene-tereftalate", Journal of Materials Science Letters, vol. 19, pp. 1843-1845, 2000.

[17] T. Meissner, F.J. Wentz, "The complex dielectric constant of pure and sea water from microwave satellite observations", IEEE Transactions Geoscience Remore Sensing, vol. 42, pp. 1836-1849, 2004.

[18] R. Patsch, "Water trees-growth and model concep", Proceedings of the 3rd International Conference on Conduction and Breakdown in Solid Dielectrics, pp. 489-493, 1989.

[19] C.T. Meyer, "Water absorption during water treeing in polyethylene", IEEE Transactions on Electrical Insulation, vol. 18, 1, pp. 28-31, 1983.

[20] R. Ross, "Inception and propagation mechanisms of water treeing", IEEE Transactions on Dielectrics and Electrical Insulation, vol. 5, 5, pp. 660-680, 1998.

[21] N. Shimizu and C. Laurent, "Electrical tree initiation", IEEE Trans.Dielectr. Electr. Insul., vol. 5, pp. 651 – 659, 1998.